A Frequency Domain Approach to Performance Optimization of High-Speed VLSI Interconnects

Ruolong Liu, Qi-Jun Zhang, *Member, IEEE,* and Michel S. Nakhla, *Senior Member, IEEE*

Abstract—**An efficient method is presented for the computation of exact group delay, gain slope and their sensitivities with respect to design parameters in multi-conductor transmission line networks. The group delay and gain slope sensitivities with respect to transmission line parameters are evaluated in terms of the second-order derivatives of the eigenvalues and eigenvectors of the propagation matrix. By combining this method with minimax optimization, a frequency-domain approach is developed to minimize transient delay and distortion in high-speed VLSI interconnects. Examples of interconnect optimization demonstrate simultaneous reductions of signal propagation delay, distortion and crosstalk at several vital connection ports. Compared to direct time domain optimization, the proposed approach is more than three times faster. The proposed technique is useful in optimal design of circuit interconnects for high-speed digital computers and communication systems.**

I. Introduction

As THE SIGNAL speed increases, the effects of VLSI interconnects such as delay, distortion and crosstalk become the dominant factor limiting the performance of the overall VLSI system. With subnanosecond rise time, the electrical length of the interconnections becomes a significant fraction of the signal wavelength. Consequently distributed and lossy transmission line models must be used. There is a recent thrust of research in the time-domain analysis of such interconnect effects, e.g., [1]–[9]. Design optimization of interconnects is addressed very recently [10], where transient responses are improved by time-domain optimization.

In this paper we present an alternative approach for optimization of transient responses such as delay, distortion and crosstalk by using frequency domain information such as group delay and gain slope.

Group delay and its sensitivities have been an attractive vehicle for circuit design such as design of filters [11]–[13] and IC digital cells [14]. Evaluation of group delay sensitivities with respect to design variables, which requires second order sensitivity analysis of the network, is necessary for gradient based optimization. However for lossy multiconductor transmission line networks, group delay sensitivity is much more involved and has not been previously presented.

The purpose of this paper is two fold. Firstly, a technique for efficient computation of exact group delay and its sensitivities is derived for multiconductor transmission line networks. Secondly, the group delay information is combined with gradient based minimax optimization to minimize delay and distortion in VLSI interconnects.

In Section II, a unified approach based on the modified nodal admittance (MNA) matrix is used to formulate network equations. Efficient computation of exact group delay, gain slope and their sensitivities for multiconductor transmission line networks is described in Section III. In Section IV a numerical example is presented to verify the proposed group delay sensitivity formulas. In Section V a frequency-domain formulation for minimization of delay and distortion in VLSI interconnects is proposed. Three numerical examples are presented in Section VI, illustrating the principles of frequency-domain interconnect optimization.

II. Network Equations with Multiconductor Transmission Lines

The admittance matrix of a multiconductor transmission line required in a modified nodal equation of the overall circuit has been described in detail in [1]. Suppose the network π consists of lumped elements and N_s multiconductor transmission lines. The modified nodal equations [15] for the overall network π are

$$\boldsymbol{C}_\pi \frac{d\boldsymbol{v}_\pi(t)}{dt} + \boldsymbol{G}_\pi \boldsymbol{v}_\pi(t) + \sum_{k=1}^{N_s} \boldsymbol{D}_k \boldsymbol{i}_k(t) = \boldsymbol{e}_\pi(t), \quad (1)$$

where $\boldsymbol{C}_\pi$ and $\boldsymbol{G}_\pi$ are N_π by N_π matrices determined by lumped elements in the network. $\boldsymbol{v}_\pi(t)$ is the vector of node voltage waveforms appended by independent voltage source current and inductor current waveforms. $\boldsymbol{D}_k$ is an incidence matrix containing 1's and 0's which maps $\boldsymbol{i}_k(t)$, the terminal current waveforms of the kth distributed transmission line, into the N_π-node space of network π. $\boldsymbol{e}_\pi(t)$ is the vector of source waveforms.

Manuscript received March 31, 1992; revised August 3, 1992. This work was supported through the Computer-Aided Engineering Chairs funded by Bell-Northern Research and the Natural Sciences and Engineering Research Council of Canada.

The authors are with the Department of Electronics, Carleton University, Ottawa, Canada K1S 5B6.

IEEE Log Number 9203708.

The s-domain equation is obtained by taking Laplace transform of (1)

$$\boldsymbol{Y}_\pi \boldsymbol{V}_\pi(s) = \boldsymbol{E}_\pi(s) + \boldsymbol{C}_\pi \boldsymbol{v}_\pi(0), \tag{2}$$

where

$$\boldsymbol{Y}_\pi = \boldsymbol{G}_\pi + s\boldsymbol{C}_\pi + \sum_{k=1}^{N_s} \boldsymbol{D}_k \boldsymbol{A}_k \boldsymbol{D}_k^T, \tag{3}$$

T denotes transpose and $\boldsymbol{A}_k$ is the nodal admittance matrix of the kth distributed transmission line.

The lossy multiconductor transmission line is assumed to be uniform along its length with an arbitrary cross section. The cross section of an N_k-conductor transmission line can be described by the following N_k by N_k matrices of line parameters: the resistance per unit length $\boldsymbol{R}$, the inductance per unit length $\boldsymbol{L}$, the capacitance per unit length $\boldsymbol{C}$ and the conductance per unit length $\boldsymbol{G}$. These matrices can be computed from physical/geometrical parameters of the transmission line through quasi-static analysis [16], [17] or empirical formulas [18]. Let γ_i^2 be an eigenvalue of the matrix $\boldsymbol{Z}_L \boldsymbol{Y}_L$ with an associated eigenvector $\boldsymbol{x}_i$, where $\boldsymbol{Z}_L = \boldsymbol{R} + s\boldsymbol{L}$ and $\boldsymbol{Y}_L = \boldsymbol{G} + s\boldsymbol{C}$. The admittance matrix for the multiconductor transmission line is [1]

$$\boldsymbol{A}_k = \begin{bmatrix} \boldsymbol{S}_i \boldsymbol{E}_1 \boldsymbol{S}_v^{-1} & \boldsymbol{S}_i \boldsymbol{E}_2 \boldsymbol{S}_v^{-1} \\ \boldsymbol{S}_i \boldsymbol{E}_2 \boldsymbol{S}_v^{-1} & \boldsymbol{S}_i \boldsymbol{E}_1 \boldsymbol{S}_v^{-1} \end{bmatrix}, \tag{4}$$

where

$$\boldsymbol{E}_1 = \text{diag}\ \{(1 + e^{-2\gamma_i l})/(1 - e^{-2\gamma_i l}), \quad i = 1, 2, \cdots, N_k\}, \tag{5}$$

$$\boldsymbol{E}_2 = \text{diag}\ \{2/(e^{-\gamma_i l} - e^{\gamma_i l}), i = 1, 2, \cdots, N_k\}, \tag{6}$$

and l is the length of the transmission line. $\boldsymbol{S}_v$ is a matrix containing all eigenvectors x_i, $i = 1, 2, \cdots, N_k$. $\boldsymbol{\Gamma}$ is a diagonal matrix with $\Gamma_{i,i} = \gamma_i$, and $\boldsymbol{S}_i = \boldsymbol{Z}_L^{-1} \boldsymbol{S}_v \boldsymbol{\Gamma}$.

III. Computation of Exact Group Delay, Gain Slope and Their Sensitivities

A. Computation of Group Delay and Gain Slope

Let

$$V_{\text{out}}(s) = \boldsymbol{u}^T \boldsymbol{V}_\pi(s) \tag{7}$$

be the frequency response of interest, where $\boldsymbol{u}$ is a constant N_π-vector and $s = j\omega$. Let θ be the phase of V_{out}. Group delay can be defined as [11]–[12]

$$T_G \triangleq -\frac{\partial \theta}{\partial \omega} = -\text{Real}\left\{\frac{1}{V_{\text{out}}} \frac{\partial V_{\text{out}}}{\partial s}\right\} \tag{8}$$

and gain slope can be defined as [13]

$$G_L \triangleq \frac{\partial 20 \log |V_{\text{out}}|}{\partial \omega} = -\frac{20}{\ln 10} \text{Imag}\left\{\frac{1}{V_{\text{out}}} \frac{\partial V_{\text{out}}}{\partial s}\right\}. \tag{9}$$

Computation of group delay and gain slope requires first-order sensitivity analysis of the network. To compute $\partial V_{\text{out}}/\partial s$, we use the adjoint sensitivity approach [11]–[12],

$$\frac{\partial V_{\text{out}}}{\partial s} = (\boldsymbol{V}_\pi^a)^T \left[\frac{\partial \boldsymbol{Y}_\pi}{\partial s} \boldsymbol{V}_\pi - \frac{\partial \boldsymbol{E}_\pi}{\partial s}\right] = (\boldsymbol{V}_\pi^a)^T \left[\left(\boldsymbol{C}_\pi + \sum_{k=1}^{N_s} \boldsymbol{D}_k \frac{\partial \boldsymbol{A}_k}{\partial s} \boldsymbol{D}_k^T\right) \boldsymbol{V}_\pi - \frac{\partial \boldsymbol{E}_\pi}{\partial s}\right], \tag{10}$$

where $\boldsymbol{V}_\pi^a$ is solved from the adjoint equation:

$$\boldsymbol{Y}_\pi^T \boldsymbol{V}_\pi^a = -\boldsymbol{u}. \tag{11}$$

To compute $\partial \boldsymbol{A}_k/\partial s$, we first compute the sensitivities of eigenvalues γ_i^2 and eigenvectors $\boldsymbol{x}_i$ w.r.t. frequency s by solving the linear equation:

$$\boldsymbol{B}\begin{bmatrix} \frac{\partial \boldsymbol{x}_i}{\partial s} \\ \frac{\partial \gamma_i^2}{\partial s} \end{bmatrix} = \begin{bmatrix} \frac{\partial (\boldsymbol{Z}_L \boldsymbol{Y}_L)}{\partial s} \boldsymbol{x}_i \\ 0 \end{bmatrix}, \tag{12}$$

where

$$\boldsymbol{B} = \begin{bmatrix} \gamma_i^2 \boldsymbol{U} - \boldsymbol{Z}_L \boldsymbol{Y}_L & \boldsymbol{x}_i \\ \boldsymbol{x}_i^T & 0 \end{bmatrix}. \tag{13}$$

The solution of (12) forms $\partial \boldsymbol{S}_v/\partial s$ and $\partial \boldsymbol{\Gamma}/\partial s$. The sensitivity $\partial \boldsymbol{A}_k/\partial s$ is then computed from

$$\frac{\partial \boldsymbol{A}_k}{\partial s}\begin{bmatrix} \boldsymbol{S}_v & 0 \\ 0 & \boldsymbol{S}_v \end{bmatrix} = \begin{bmatrix} \frac{\partial \boldsymbol{S}_i}{\partial s} & 0 \\ 0 & \frac{\partial \boldsymbol{S}_i}{\partial s} \end{bmatrix} \begin{bmatrix} \boldsymbol{E}_1 & \boldsymbol{E}_2 \\ \boldsymbol{E}_2 & \boldsymbol{E}_1 \end{bmatrix} + \begin{bmatrix} \boldsymbol{S}_i & 0 \\ 0 & \boldsymbol{S}_i \end{bmatrix} \begin{bmatrix} \frac{\partial \boldsymbol{E}_1}{\partial s} & \frac{\partial \boldsymbol{E}_2}{\partial s} \\ \frac{\partial \boldsymbol{E}_2}{\partial s} & \frac{\partial \boldsymbol{E}_1}{\partial s} \end{bmatrix} - \boldsymbol{A}_k \begin{bmatrix} \frac{\partial \boldsymbol{S}_v}{\partial s} & 0 \\ 0 & \frac{\partial \boldsymbol{S}_v}{\partial s} \end{bmatrix}, \tag{14}$$

where $\partial \boldsymbol{S}_i/\partial s$ is obtained from

$$\boldsymbol{Z}_L \frac{\partial \boldsymbol{S}_i}{\partial s} = \frac{\partial \boldsymbol{S}_v}{\partial s} \boldsymbol{\Gamma} + \boldsymbol{S}_v \frac{\partial \boldsymbol{\Gamma}}{\partial s} - \frac{\partial \boldsymbol{Z}_L}{\partial s} \boldsymbol{S}_i. \tag{15}$$

B. Computation of Group Delay and Gain Slope Sensitivities

Let ϕ be a design variable. In order to obtain the sensitivity of group delay, we differentiate (8)

$$\frac{\partial T_G}{\partial \phi} = \text{Real}\left\{\frac{1}{V_{\text{out}}^2} \frac{\partial V_{\text{out}}}{\partial \phi} \frac{\partial V_{\text{out}}}{\partial s} - \frac{1}{V_{\text{out}}} \frac{\partial^2 V_{\text{out}}}{\partial s \partial \phi}\right\}. \tag{16}$$

Similarly, by differentiating (9), we have

$$\frac{\partial G_L}{\partial \phi} = \frac{20}{\ln 10} \operatorname{Imag}\left\{ \frac{1}{V_{\text{out}}^2} \frac{\partial V_{\text{out}}}{\partial \phi} \frac{\partial V_{\text{out}}}{\partial s} - \frac{1}{V_{\text{out}}} \frac{\partial^2 V_{\text{out}}}{\partial s \partial \phi} \right\}. \tag{17}$$

Therefore both group delay sensitivity and gain slope sensitivity require first- and second-order derivative information $\partial V_{\text{out}}/\partial s$, $\partial V_{\text{out}}/\partial \phi$ and $\partial^2 V_{\text{out}}/\partial s \partial \phi$.

Similar to computing $\partial V_{\text{out}}/\partial s$, the sensitivity $\partial V_{\text{out}}/\partial \phi$ can be calculated from [2]

$$\frac{\partial V_{\text{out}}}{\partial \phi} = (\boldsymbol{V}_\pi^a)^T \left[\left(\frac{\partial \boldsymbol{G}_\pi}{\partial \phi} + s \frac{\partial \boldsymbol{C}_\pi}{\partial \phi} + \sum_{k=1}^{N_s} \boldsymbol{D}_k \frac{\partial \boldsymbol{A}_k}{\partial \phi} \boldsymbol{D}_k^T \right) \cdot \boldsymbol{V}_\pi - \frac{\partial \boldsymbol{C}_k}{\partial \phi} \boldsymbol{v}_\pi(0) \right], \tag{18}$$

where

$$\frac{\partial \boldsymbol{A}_k}{\partial \phi} \begin{bmatrix} \boldsymbol{S}_v & 0 \\ 0 & \boldsymbol{S}_v \end{bmatrix} = \begin{bmatrix} \dfrac{\partial \boldsymbol{S}_i}{\partial \phi} & 0 \\ 0 & \dfrac{\partial \boldsymbol{S}_i}{\partial \phi} \end{bmatrix} \begin{bmatrix} \boldsymbol{E}_1 & \boldsymbol{E}_2 \\ \boldsymbol{E}_2 & \boldsymbol{E}_1 \end{bmatrix} + \begin{bmatrix} \boldsymbol{S}_i & 0 \\ 0 & \boldsymbol{S}_i \end{bmatrix} \begin{bmatrix} \dfrac{\partial \boldsymbol{E}_1}{\partial \phi} & \dfrac{\partial \boldsymbol{E}_2}{\partial \phi} \\ \dfrac{\partial \boldsymbol{E}_2}{\partial \phi} & \dfrac{\partial \boldsymbol{E}_1}{\partial \phi} \end{bmatrix} - \boldsymbol{A}_k \begin{bmatrix} \dfrac{\partial \boldsymbol{S}_v}{\partial \phi} & 0 \\ 0 & \dfrac{\partial \boldsymbol{S}_v}{\partial \phi} \end{bmatrix}, \tag{19}$$

$$\boldsymbol{Z}_L \frac{\partial \boldsymbol{S}_i}{\partial \phi} = \frac{\partial \boldsymbol{S}_v}{\partial \phi} \boldsymbol{\Gamma} + \boldsymbol{S}_v \frac{\partial \boldsymbol{\Gamma}}{\partial \phi} - \frac{\partial \boldsymbol{Z}_L}{\partial \phi} \boldsymbol{S}_i, \tag{20}$$

$$\boldsymbol{B} \begin{bmatrix} \dfrac{\partial \boldsymbol{x}_i}{\partial \phi} \\ \dfrac{\partial \gamma_i^2}{\partial \phi} \end{bmatrix} = \begin{bmatrix} \dfrac{\partial (\boldsymbol{Z}_L \boldsymbol{Y}_L)}{\partial \phi} \boldsymbol{x}_i \\ 0 \end{bmatrix}. \tag{21}$$

Now the problem is to find second-order derivative $\partial^2 V_{\text{out}}/\partial s \partial \phi$. Differentiating (10), we have

$$\frac{\partial^2 V_{\text{out}}}{\partial s \partial \phi} = \frac{\partial (\boldsymbol{V}_\pi^a)^T}{\partial \phi} \left[\frac{\partial \boldsymbol{Y}_\pi}{\partial s} \boldsymbol{V}_\pi - \frac{\partial \boldsymbol{E}_\pi}{\partial s} \right] + (\boldsymbol{V}_\pi^a)^T \left[\frac{\partial^2 \boldsymbol{Y}_\pi}{\partial s \partial \phi} \boldsymbol{V}_\pi + \frac{\partial \boldsymbol{Y}_\pi}{\partial s} \frac{\partial \boldsymbol{V}_\pi}{\partial \phi} \right], \tag{22}$$

where the sensitivity of adjoint response is solved from

$$\boldsymbol{Y}_\pi^T \frac{\partial \boldsymbol{V}_\pi^a}{\partial \phi} = -\frac{\partial (\boldsymbol{Y}_\pi^T)}{\partial \phi} \boldsymbol{V}_\pi^a \tag{23}$$

and the second-order sensitivity of $\boldsymbol{Y}_\pi$ is

$$\frac{\partial^2 \boldsymbol{Y}_\pi}{\partial s \partial \phi} = \frac{\partial \boldsymbol{C}_\pi}{\partial \phi} + \sum_{k=1}^{N_s} \boldsymbol{D}_k \frac{\partial^2 \boldsymbol{A}_k}{\partial s \partial \phi} \boldsymbol{D}_k^T. \tag{24}$$

Now it is necessary to compute the second-order derivative $\partial^2 \boldsymbol{A}_k/\partial s \partial \phi$ for multiconductor transmission lines. For this purpose, the calculation of the second-order derivatives of eigenvalues and eigenvectors is required. From (12), we have

$$\boldsymbol{B} \begin{bmatrix} \dfrac{\partial^2 \boldsymbol{x}_i}{\partial s \partial \phi} \\ \dfrac{\partial^2 \gamma_i^2}{\partial s \partial \phi} \end{bmatrix} = \begin{bmatrix} \dfrac{\partial^2 (\boldsymbol{Z}_L \boldsymbol{Y}_L)}{\partial s \partial \phi} \boldsymbol{x}_i + \dfrac{\partial (\boldsymbol{Z}_L \boldsymbol{Y}_L)}{\partial s} \dfrac{\partial \boldsymbol{x}_i}{\partial \phi} \\ 0 \end{bmatrix} - \frac{\partial \boldsymbol{B}}{\partial \phi} \begin{bmatrix} \dfrac{\partial \boldsymbol{x}_i}{\partial s} \\ \dfrac{\partial \gamma_i^2}{\partial s} \end{bmatrix}, \tag{25}$$

where $\partial \boldsymbol{B}/\partial \phi$ contains first-order sensitivities $\partial \gamma_i^2/\partial \phi$, $\partial \boldsymbol{x}_i/\partial \phi$ and $\partial (\boldsymbol{Z}_L \boldsymbol{Y}_L)/\partial \phi$ which have already been solved in calculating $\partial V_{\text{out}}/\partial \phi$. The solution of the linear equations (25) needs only forward and backward substitutions since the LU factors of $\boldsymbol{B}$ are available from solving (12).

Once we have $\partial^2 \boldsymbol{x}_i/\partial s \partial \phi$ and $\partial^2 \gamma_i^2/\partial s \partial \phi$, we can easily obtain $\partial^2 \boldsymbol{S}_v/\partial s \partial \phi$ and $\partial^2 \boldsymbol{\Gamma}/\partial s \partial \phi$. Finally from (14), $\partial^2 \boldsymbol{A}_k/\partial s \partial \phi$ can be solved from

$$\begin{aligned} \frac{\partial^2 \boldsymbol{A}_k}{\partial s \partial \phi} \begin{bmatrix} \boldsymbol{S}_v & 0 \\ 0 & \boldsymbol{S}_v \end{bmatrix} &= \begin{bmatrix} \dfrac{\partial^2 \boldsymbol{S}_i}{\partial s \partial \phi} & 0 \\ 0 & \dfrac{\partial^2 \boldsymbol{S}_i}{\partial s \partial \phi} \end{bmatrix} \begin{bmatrix} \boldsymbol{E}_1 & \boldsymbol{E}_2 \\ \boldsymbol{E}_2 & \boldsymbol{E}_1 \end{bmatrix} \\ &+ \begin{bmatrix} \dfrac{\partial \boldsymbol{S}_i}{\partial s} & 0 \\ 0 & \dfrac{\partial \boldsymbol{S}_i}{\partial s} \end{bmatrix} \begin{bmatrix} \dfrac{\partial \boldsymbol{E}_1}{\partial \phi} & \dfrac{\partial \boldsymbol{E}_2}{\partial \phi} \\ \dfrac{\partial \boldsymbol{E}_2}{\partial \phi} & \dfrac{\partial \boldsymbol{E}_1}{\partial \phi} \end{bmatrix} \\ &+ \begin{bmatrix} \dfrac{\partial \boldsymbol{S}_i}{\partial \phi} & 0 \\ 0 & \dfrac{\partial \boldsymbol{S}_i}{\partial \phi} \end{bmatrix} \begin{bmatrix} \dfrac{\partial \boldsymbol{E}_1}{\partial s} & \dfrac{\partial \boldsymbol{E}_2}{\partial s} \\ \dfrac{\partial \boldsymbol{E}_2}{\partial s} & \dfrac{\partial \boldsymbol{E}_1}{\partial s} \end{bmatrix} \\ &+ \begin{bmatrix} \boldsymbol{S}_i & 0 \\ 0 & \boldsymbol{S}_i \end{bmatrix} \begin{bmatrix} \dfrac{\partial^2 \boldsymbol{E}_1}{\partial s \partial \phi} & \dfrac{\partial^2 \boldsymbol{E}_2}{\partial s \partial \phi} \\ \dfrac{\partial^2 \boldsymbol{E}_2}{\partial s \partial \phi} & \dfrac{\partial^2 \boldsymbol{E}_1}{\partial s \partial \phi} \end{bmatrix} - \frac{\partial \boldsymbol{A}_k}{\partial \phi} \begin{bmatrix} \dfrac{\partial \boldsymbol{S}_v}{\partial s} & 0 \\ 0 & \dfrac{\partial \boldsymbol{S}_v}{\partial s} \end{bmatrix} \\ &- \boldsymbol{A}_k \begin{bmatrix} \dfrac{\partial^2 \boldsymbol{S}_v}{\partial s \partial \phi} & 0 \\ 0 & \dfrac{\partial^2 \boldsymbol{S}_v}{\partial s \partial \phi} \end{bmatrix} - \frac{\partial \boldsymbol{A}_k}{\partial s} \begin{bmatrix} \dfrac{\partial \boldsymbol{S}_v}{\partial \phi} & 0 \\ 0 & \dfrac{\partial \boldsymbol{S}_v}{\partial \phi} \end{bmatrix}, \end{aligned} \tag{26}$$

where $\partial^2 \boldsymbol{S}_t / \partial s \partial \phi$ is obtained from

$$\boldsymbol{Z}_L \frac{\partial^2 \boldsymbol{S}_t}{\partial s \partial \phi} = \frac{\partial^2 \boldsymbol{S}_{t'}}{\partial s \partial \phi} \boldsymbol{\Gamma} + \frac{\partial \boldsymbol{S}_{t'}}{\partial s} \frac{\partial \boldsymbol{\Gamma}}{\partial \phi} + \frac{\partial \boldsymbol{S}_{t'}}{\partial \phi} \frac{\partial \boldsymbol{\Gamma}}{\partial s} + \boldsymbol{S}_{t'} \frac{\partial^2 \boldsymbol{\Gamma}}{\partial s \partial \phi} - \frac{\partial^2 \boldsymbol{Z}_L}{\partial s \partial \phi} \boldsymbol{S}_t - \frac{\partial \boldsymbol{Z}_L}{\partial s} \frac{\partial \boldsymbol{S}_t}{\partial \phi} - \frac{\partial \boldsymbol{Z}_L}{\partial \phi} \frac{\partial \boldsymbol{S}_t}{\partial s}. \tag{27}$$

IV. Verification of Group Delay Sensitivity Formulas

The formulas for calculating group delay, gain slope and their sensitivities are implemented in a program for the design of distributed networks with lossy coupled transmission lines. Consider the 3 transmission line example of Fig. 1. The lengths of the 3 transmission lines are 0.05 m, 0.04 m and 0.03 m, respectively. The cross-sectional physical parameters are conductor width w = 0.00058 m, circuit board thickness h = 0.00117 m, distance between the two conductors d = 0.00249 m and relative dielectric constant ϵ_r = 4.54. The empirical formulas from [18] is used to compute the $\boldsymbol{R}$, $\boldsymbol{L}$, $\boldsymbol{G}$ and $\boldsymbol{C}$ matrices for the transmission lines. Group delay sensitivities computed from the new formulas in Section III are compared with that from the perturbation in Fig. 2. Excellent agreement is observed. Computation speed by the new formulas is faster than by perturbation. In the perturbation method frequency ω and variable ϕ are perturbed by a small amount, $\Delta\omega$ and $\Delta\phi$, respectively. The network equations are resolved at perturbed points of ω and ϕ. The group delay sensitivity is found using finite difference approximation. The perturbation method requires at least three analyses to the original circuit for each variable under consideration. But by using the proposed method, only one circuit analysis plus small additional computational cost is needed to get the sensitivities with respect to all variables. Notice that no LU factorization is required for solving (11) and (23), only forward/backward substitutions being needed. Similarly only forward/backward substitutions are required for solving (21) and (25). Since $\boldsymbol{A}_k$, $\boldsymbol{B}$, $\boldsymbol{E}_1$, $\boldsymbol{E}_2$, $\boldsymbol{S}_t$ and $\boldsymbol{S}_{t'}$ are all relatively small matrices, the computational effort for solving (12), (14), (19), (25) and (26) is small compared with a large circuit simulation.

V. Proposed Formulation of VLSI Interconnect Optimization

It is well known that the group delay contains information of signal propagation delay. For RC networks Vlach *et al.* recently verified group delay at frequency zero as being exactly equal to Elmore delay and observed a simple empirical relation between group delay and signal delay of responses corresponding to a step excitation [14]. In general, over a frequency range of interest, the smaller the group delay, the smaller the signal propagation delay. Furthermore, if an output is a delayed replica of the input, flat group delay and zero gain slope should hold across the entire frequency range. We take advantage of group delay and gain slope information for reduction of the transient signal propagation delay and distortion in a distributed network environment. The actual optimization is performed in frequency domain.

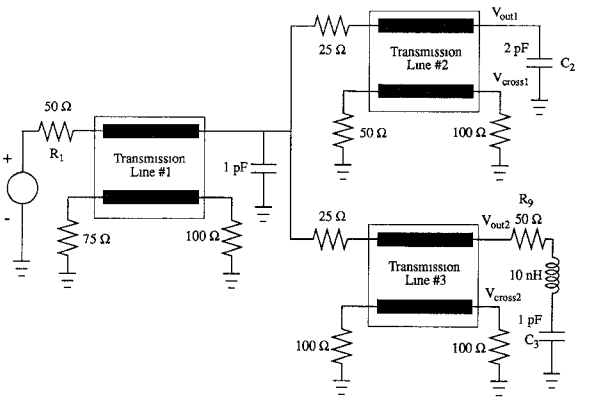

Fig. 1. Circuit schematic for the 3 transmission line network example.

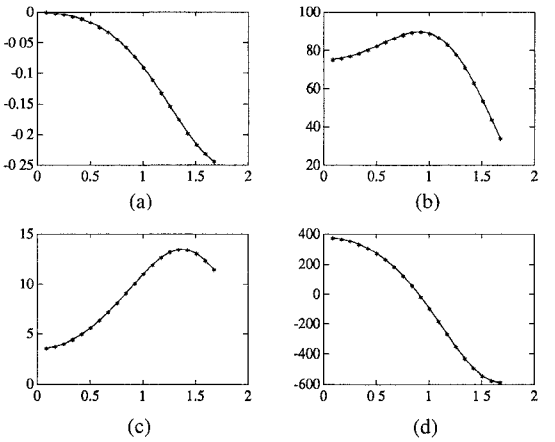

Fig. 2. The 3 transmission line example. Sensitivity of group delay versus angular frequency (10^9 rad/s) by proposed method (solid line) and by perturbation method (the stars). (a) Sensitivity w.r.t. R_9, (b) Sensitivity w.r.t. C_2, (c) Sensitivity w.r.t. the length of transmission line 1 and (d) Sensitivity w.r.t. the conductor width of all transmission lines.

A. Error Functions

Let Φ denote all design variables including physical/geometrical parameters of the transmission lines and parameters in termination/matching networks. Let $S_{G,u}(s)$ and $S_{G,l}(s)$ be upper and lower specifications on group delay T_G, respectively. Let W_G be a positive weighting factor. The minimization of signal delay can be achieved by minimizing

$$W_G(T_G(\Phi, s_k) - S_{G.u}(s_k)) \tag{28}$$

over a range of frequencies, $s_k = j\omega_k$, $k = 1, 2, \cdots, K$. By imposing a lower specification on group delay, we have an error function

$$-W_G(T_G(\Phi, s_k) - S_{G,l}(s_k)). \tag{29}$$

A typical lower specification is $S_{G.l}(s) = 0$. Simultaneous minimization of (28) and (29) over a frequency range reduces the group delay and improves its flatness.

Let $F(\Phi, s)$ be the transfer function of the network. Let $S_{F,l}(s)$ be the lower specification on the magnitude of $F(\Phi, s)$ and $S_L(s)$ be the upper specification on the magnitude of gain slope. Let W_F and W_L be positive weighting factors. Minimizing the following error functions

$$-W_F[|F(\Phi, s_k)| - S_{F,l}(s_k)] \tag{30}$$

$$W_L[G_L(\Phi, s_k) - S_L(s_k)] \tag{31}$$

$$-W_L[G_L(\Phi, s_k) + S_L(s_k)] \tag{32}$$

over a frequency range increases signal level and flatness of the transfer function magnitude. A flat group delay and flat magnitude of the transfer function reduces signal distortion.

Let $V(\Phi, s)$ be the spectrum of crosstalk waveform. Reduction of crosstalk is realized by minimizing the magnitude of $V(\Phi, s)$ using

$$W_C(|V(\Phi, s_k)| - S_C(s_k)), \tag{33}$$

where S_C is the specification on the magnitude of spectrum $V(\Phi, s)$ and W_C is a positive weighting factor.

B. Selection of Frequencies

The range of frequencies is determined by the fundamental frequency and its significant harmonics of the input signal. To find an approximate fundamental frequency for a trapezoidal signal excitation, we first select a time interval T long enough such that the transient will effectly vanish within T, and then choose $2\pi/T$ as the fundamental angular frequency ω_1. To cover the dominate transient, generally 20–25 harmonics need to be considered [6].

It should be pointed out that by optimizing only the dominant components of the transient responses, we achieve CPU speedup over time domain optimization. Final transient responses can be accurately obtained by using time domain simulators after optimization converges.

C. Selection of Optimization Variables

The overall circuit performance is affected by parameters in both the interconnections and their terminations. The terminations typically represent basic circuit blocks and matching networks. There are two stages of interconnect design. In the first stage, the length of the transmission line l, the distance between the couped conductors d, and the width of the conductors w can be optimized. The thickness of PCB layer h is typically selected from a set of standard values. In the second design stage only the length l is optimizable. A different design scenario is to find optimal termination parameters for a given interconnect configuration. In this way, the interconnect network can be optimally matched and signal reflections and distortions are effectively reduced.

D. Formulation of Optimization

Let $\boldsymbol{e}(\Phi)$ be an m-vector containing all necessary error functions as defined by (28)–(33). The optimization problem is to find Φ such that

$$U(\Phi) \triangleq \max_j \{e_j(\Phi), j = 1, 2, \cdots, m\} \tag{34}$$

is minimized subject to electrical and physical constraints $\mathbf{g}(\Phi) \leq \mathbf{0}$ and $\boldsymbol{h}(\Phi) = \mathbf{0}$. The constraints represent design rules. For example the total length of several interconnect lines must be constrained by the physical dimensions of the circuit board. The total separation between several coupled conductors must be limited by the geometrical space available to them. The minimax optimization of (34) is solved by a gradient-based two stage minimax algorithm [19], [20]. The derivatives of $\boldsymbol{e}$ with respect to Φ required by the optimizer are obtained by the new approach of first- and second-order sensitivity analysis described in Section III.

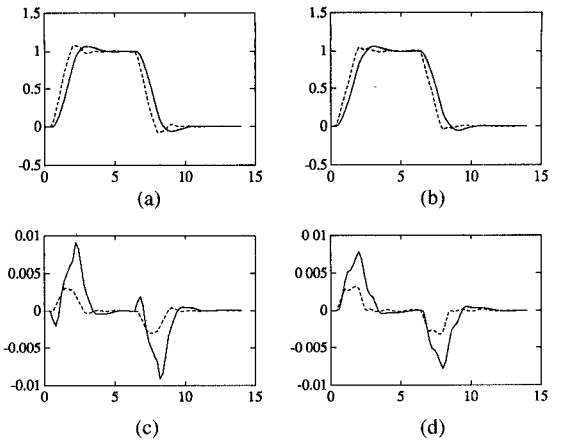

Fig. 3. The 3 transmission line example. Transient responses (volts) versus time (ns) before (solid line) and after (dashed line) frequency domain optimization. (a) V_{out1}, (b) V_{out2}, (c) V_{cross1} and (d) V_{cross2}.

VI. Examples

Example 1: A 3 Transmission Line Network

The circuit of Fig. 1 is excited by an 1V pulse with 1.5 ns rise/fall time and 4 ns duration. The time responses before optimization are plotted in Fig. 3. The objective is to reduce signal delay of V_{out1} and V_{out2}, and the crosstalk voltages V_{cross1} and V_{cross2}, respectively. Design variables Φ include capacitors C_2 and C_3, resistor R_9, lengths of the three transmission lines l_1, l_2 and l_3, distance between the 2 conductors d and the width of the conductors w. The cross-sectional parameters are common among the 3 transmission lines. The initial values are

$$\Phi = [l_1 \quad l_2 \quad l_3 \quad d \quad w \quad C_2 \quad C_3 \quad R_9]^T$$
$$= [50 \quad 40 \quad 30 \quad 2.49 \quad 0.58 \quad 2 \quad 1 \quad 50]^T,$$

where the unit for length, width and distance is mm. The units for capacitors and resisters are pF and Ω, respectively. We require that the total length of the three transmission lines be fixed at 120 mm and the width of each conductor plus the spacing between them be fixed at 3.07

mm. This results in constraints

$$h_1(\Phi) = l_1 + l_2 + l_3 - 120 = 0.$$

$$h_2(\Phi) = w + d - 3.07 = 0.$$

Fig. 4 shows frequency domain specifications and responses for group delay at two outputs, namely, $T_{G,\text{out1}}$ and $T_{G,\text{out2}}$ and crosstalk spectrums V_{cross1} and V_{cross2}. The error functions used in (34) are

$$\boldsymbol{e} = \begin{bmatrix} e_1 \\ \vdots \\ e_{20} \\ e_{21} \\ \vdots \\ e_{40} \\ e_{41} \\ \vdots \\ e_{60} \\ e_{61} \\ \vdots \\ e_{80} \end{bmatrix} = \begin{bmatrix} T_{G,\text{out1}}(\Phi, s_1) - 0.5 \\ \vdots \\ T_{G,\text{out1}}(\Phi, s_{20}) - 0.5 \\ T_{G,\text{out2}}(\Phi, s_1) - 0.5 \\ \vdots \\ T_{G,\text{out2}}(\Phi, s_{20}) - 0.5 \\ 1000(|V_{\text{cross1}}(\Phi, s_1)| - 0.00028) \\ \vdots \\ 1000(|V_{\text{cross1}}(\Phi, s_{20})| - 0.00028) \\ 1000(|V_{\text{cross2}}(\Phi, s_1)| - 0.00028) \\ \vdots \\ 1000(|V_{\text{cross2}}(\Phi, s_{20})| - 0.00028) \end{bmatrix}.$$

where $s_k = jk\omega_k = jk\omega_1$, $k = 1, 2, \cdots, 20$ and $\omega_1 = 0.0837758 \times 10^9$ rad/sec. The total number of error functions is 80. The total number of linear constraints is 10, including bounds on the design variables. After optimization, the objective function (34) is reduced from 1.0134 to -0.0386, indicating that all specifications are satisfied. The variables after optimization are

$$\Phi = [98.38 \;\; 11.62 \;\; 10 \;\; 2.97 \;\; 0.1 \;\; 0.1 \;\; 8.884 \;\; 197.8]^T.$$

The group delay after optimization, as plotted in Fig. 4, is much lower and flatter than before optimization. Time responses after optimization are plotted against those before optimization in Fig. 3. The propagation delay times for V_{out1} and V_{out2} are both reduced from 1.6 ns to 1.2 ns. The magnitude of crosstalk signals V_{cross1} and V_{cross2} is reduced by more than 55%.

Example 2: 25 Transmission Line Network

The circuit of Fig. 5 represents a 4-bit bus structure in which the excitation signals propagate through the bus lines to various circuit blocks. The 13 4-conductor transmission lines have the same cross-sectional geometry. Both excitations are 5 V pulses with 1 ns rise/fall time and 5 ns duration. The responses of interests are V_a, V_b, V_c, and V_d, as shown in Fig. 6.

Design specifications include upper specifications on the group delay and lower specifications on the magnitudes of transfer functions, respectively, for both output V_b and V_d. Upper specifications are also placed on the spectrums of crosstalk signals of V_a and V_c, as shown in Fig. 7. The total number of error functions is 120. There are 27 design variables in Φ consisting of parameters in both the transmission lines and the termination networks,

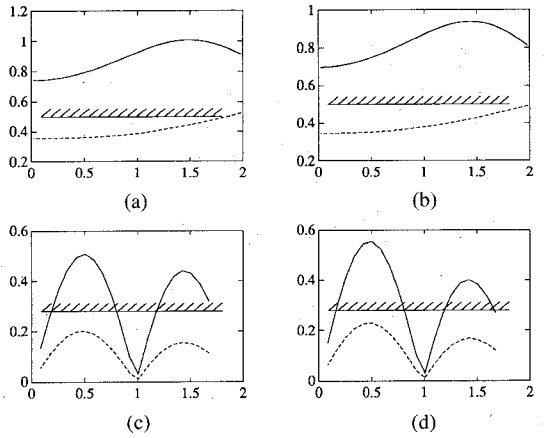

Fig. 4. The 3 transmission line example. Frequency domain specifications and group delay and spectrum responses versus angular frequency (10^9 rad/s) before (solid line) and after (dashed line) optimization. (a) T_G for V_{out1}, (b) T_G for V_{out2}, (c) Spectrum for V_{cross1} (mV) and (d) Spectrum for V_{cross2} (mV).

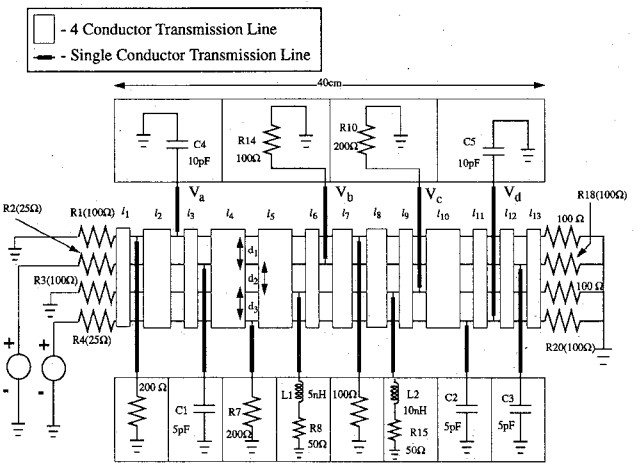

Fig. 5. Circuit diagram for the 25 transmission line network example. There are 13 4-conductor coupled transmission lines and 12 single conductor transmission lines. Two excitations are simultaneously applied.

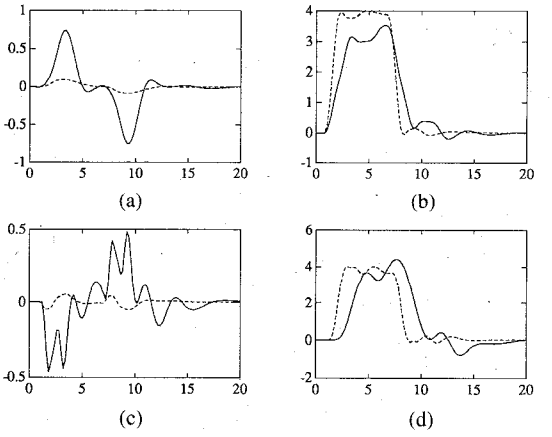

Fig. 6. The 25 transmission line example. Transient responses (volts) versus time (ns) before (solid line) and after (dashed line) frequency domain optimization. (a) V_a, (b) V_b, (c) V_c and (d) V_d.

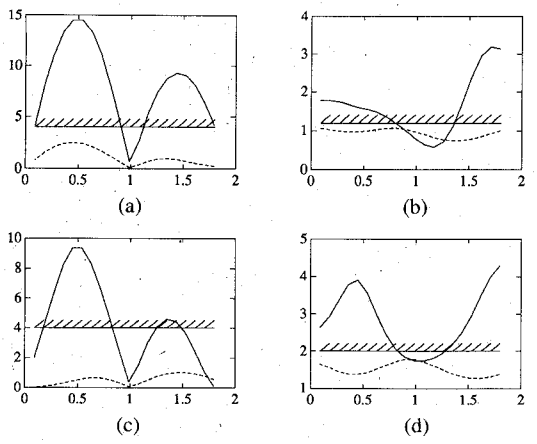

Fig. 7. The 25 transmission line example. Frequency domain specifications and group delay and spectrum responses versus angular frequency (10^9 rad/s) before (solid line) and after (dashed line) optimization. (a) Spectrum for V_a (mV), (b) T_G for V_b, (c) Spectrum for V_c (mV) and (d) T_G for V_d.

as listed in Table I. The total number of linear constraints is 43.

After 12 iterations of optimization, the objective function (34) was reduced from 22.908 to -1.177. The group delay after optimization is lower and flatter as shown in Fig. 7. The parameters before and after optimization are listed in Table I. The output responses V_a, V_b, V_c, and V_d after optimization are plotted against those before optimization in Fig. 6. The propagation delay times of V_b and V_d are reduced from 2.5 and 3.9 ns down to 1.5 ns and 2.1 ns, respectively based on 2 V threshold criteria. The peaks of crosstalk voltages V_a and V_c are reduced to 0.09 and 0.05 V, respectively. In addition, the reflection in the output response V_d is significantly smaller than before optimization. The rise/fall time of signal V_b is also improved.

In order to compare our new approach with direct time-domain optimization [10], we also performed optimization explicitly on the time waveform of this example. Comparable results were obtained. However, the CPU times for our approach and the direct time domain approach are 4519 and 15410 seconds (on SPARCstation 2), respectively. Our proposed approach is 3.4 times faster than direct time-domain optimization.

We also performed optimization with only termination parameters as design variables. After optimization, the crosstalk and the distortion of the signals were significantly improved. There was no substantial change in signal propagation delay because the transmission lines were fixed.

Example 3: Multi-Circuit Optimization

The simultaneous optimization of the circuit in Fig. 6, namely Circuit 1, and its modified version, namely Circuit 2, is performed. Circuit 2 is identical to Circuit 1 except that the excitations are applied through R_1 and R_3. The 34 optimization variables as listed in Table II are common between the two circuits. This multi-circuit optimization example represents optimal design of such interconnect structure for two different and conflicting cases of signal propagation.

TABLE I
OPTIMIZATION VARIABLES FOR THE 25 TRANSMISSION LINE EXAMPLE

Var.	Before Opt.	After Opt.	Var.	Before Opt.	After Opt.
l_1	0.025 m	0.026788 m	d_2	1.0 mm	1.325 mm
l_2	0.035 m	0.049477 m	d_3	1.0 mm	0.8 mm
l_3	0.025 m	0.01 m	R_2	25 Ω	18.9 Ω
l_4	0.04 m	0.010296 m	R_4	25 Ω	20.4 Ω
l_5	0.04 m	0.033452 m	R_7	200 Ω	1067.3 Ω
l_6	0.025 m	0.01 m	R_{10}	200 Ω	10.0 Ω
l_7	0.035 m	0.012302 m	R_{14}	100 Ω	353.2 Ω
l_8	0.035 m	0.034221 m	R_{18}	100 Ω	87.1 Ω
l_9	0.025 m	0.017584 m	R_{20}	100 Ω	78.7 Ω
l_{10}	0.04 m	0.045879 m	C_1	5 pF	0.1 pF
l_{11}	0.025 m	0.01 m	C_2	5 pF	0.1 pF
l_{12}	0.025 m	0.07 m	C_3	5 pF	0.1 pF
l_{13}	0.025 m	0.07 m	C_5	10 pF	0.1 pF
d_1	1.0 mm	2.875 mm			

TABLE II
OPTIMIZATION VARIABLES FOR THE MULTICIRCUIT EXAMPLE

Var.	Before Opt.	After Opt.	Var.	Before Opt.	After Opt.
l_1	0.025 m	0.07 m	R_2	100 Ω	50.9 Ω
l_2	0.035 m	0.07 m	R_3	100 Ω	38.8 Ω
l_3	0.025 m	0.012365 m	R_4	100 Ω	110.0 Ω
l_4	0.04 m	0.014719 m	R_7	200 Ω	499.4 Ω
l_5	0.04 m	0.015807 m	R_8	50 Ω	1245.7 Ω
l_6	0.025 m	0.012618 m	R_{10}	200 Ω	977.5 Ω
l_7	0.035 m	0.019749 m	R_{14}	100 Ω	817.8 Ω
l_8	0.035 m	0.22156 m	R_{15}	50 Ω	112.0 Ω
l_9	0.025 m	0.010761 m	R_{18}	100 Ω	94.1 Ω
l_{10}	0.04 m	0.036799 m	R_{20}	100 Ω	139.4 Ω
l_{11}	0.025 m	0.28267 m	C_1	5 pF	1.36 pF
l_{12}	0.025 m	0.28334 m	C_2	5 pF	1.721 pF
l_{13}	0.025 m	0.58425 m	C_3	5 pF	0.872 pF
d_1	1.0 mm	1.076 mm	C_4	10 pF	0.1 pF
d_2	1.0 mm	1.116 mm	C_5	10 pF	3.0 pF
d_3	1.0 mm	1.577 mm	L_1	5 nH	5.413 nH
R_1	100 Ω	39.9 Ω	L_2	10 nH	34.6 nH

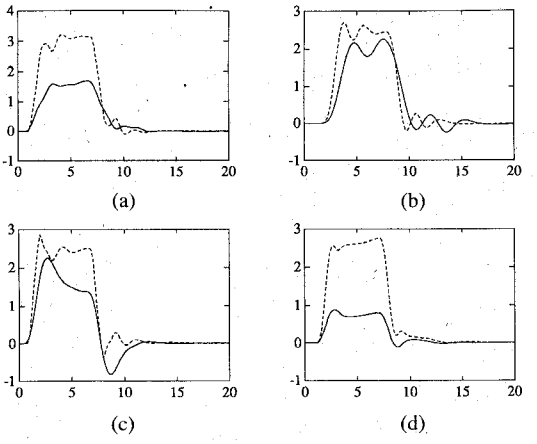

Fig. 8. The multi-circuit optimization example. Transient responses (volts) versus time (ns) before (solid line) and after (dashed line) frequency domain optimization. (a) V_b of Circuit 1, (b) V_d of Circuit 1, (c) V_a of Circuit 2 and (d) V_c of Circuit 2.

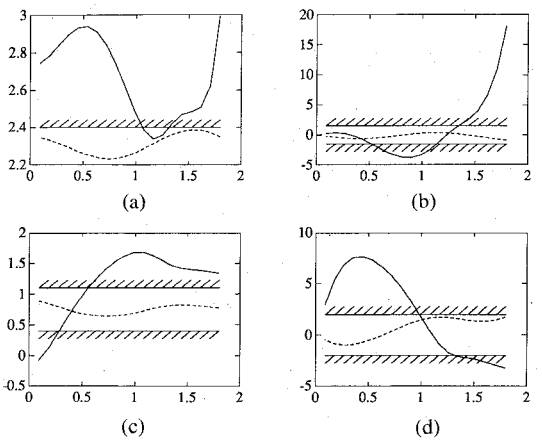

Fig. 9. The multi-circuit optimization example. Representative group delay and gain slope responses versus angular frequency (10^9 rad/s) before (solid line) and after (dashed line) optimization. (a) T_G for V_d of Circuit 1, (b) G_L for V_d of Circuit 1, (c) T_G for V_a of Circuit 2 and (d) G_L for V_a of Circuit 2.

Both upper and lower specifications are applied to group delay and gain slope responses. Lower specifications are also applied to the magnitudes of transfer functions and upper specifications to the spectrums of crosstalk signals in both Circuits 1 and 2. The total number of error functions is 380 and the number of linear constraints is 50. The time-domain and the frequency domain responses before and after optimization are plotted in Figs. 8 and 9, respectively. After optimization both group delay and gain slope responses become flatter. The magnitude of gain slope responses becomes lower. The propagation delay and distortion for both circuits are reduced. As shown in Fig. 8 the signal levels are increased and the rise/fall times of all the four signals are improved.

VII. Conclusion

An efficient method is presented for the computation of exact group delay, gain slope and their sensitivities with respect to design parameters in multiconductor transmission line networks. By combining this method with minimax optimization, a frequency-domain approach is developed to indirectly minimize delay, distortion and crosstalk of transient responses in high-speed VLSI interconnects. Compared to direct time-domain optimization, the new approach is approximate and therefore faster. It can be used as an efficient way in the design of interconnects in high-speed VLSI systems. Furthermore to obtain both efficiency and accuracy in an overall design task, the frequency-domain approach can be used in the initial design stage to achieve a near-optimal design. The time-domain approach can be used in the final stage for "fine tuning."

References

[1] R. Griffith and M. S. Nakhla, "Time-domain analysis of lossy coupled transmission lines," *IEEE Trans. Microwave Theory Tech.*, vol. 38, pp. 1480–1487, 1990.

[2] S. Lum, M. S. Nakhla, and Q. J. Zhang, "Sensitivity analysis of lossy coupled transmission lines," *IEEE Trans. Microwave Theory Tech.*, vol. 39, pp. 2089–2099, 1991.

[3] H. Hasegawa and S. Seki, "Analysis of interconnection delay on very high-speed LSI/VLSI chips using a microstrip line model," *IEEE Trans. Electron Devices*, vol. ED-31, pp. 1954–1960, 1984.

[4] F. Y. Chang, "The generalized method of characteristics for waveform relaxation analysis of lossy coupled transmission lines," *IEEE Trans. Microwave Theory Tech.*, vol. 37, pp. 2028–2038, 1989.

[5] A. R. Djordjevic and T. K. Sarkar, "Analysis of time response of lossy multiconductor transmission line networks," *IEEE Trans. Microwave Theory Tech.*, vol. MTT-35, pp. 898–908, 1987.

[6] R. A. Sainati and T. J. Moravec, "Estimating high speed circuit interconnect performance," *IEEE Trans. Circuit Syst.*, vol. 36, pp. 533–541, 1989.

[7] D. Winklestein, M. B. Steer, and R. Pomerleau, "Simulation of arbitrary transmission line networks with nonlinear terminations," *IEEE Trans. Circuits Syst.*, vol. 38, pp. 418–422, 1991.

[8] S. S. Gao, A. Y. Yang, and S. M. Kang, "Modelling and simulation of interconnection delays and crosstalk in high-speed integrated circuits," *IEEE Trans. Circuits Syst.*, vol. 37, pp. 1–9, 1990.

[9] M. S. Nakhla, "Analysis of pulse propagation on high-speed VLSI chips," *IEEE J. Solid-State Circuits*, vol. 25, pp. 490–494, 1990.

[10] Q. J. Zhang, S. Lum, M. S. Nakhla, "Minimization of delay and crosstalk in high-speed VLSI interconnects," *IEEE Trans. Microwave Theory Tech.*, vol. 40, pp. 1555–1563, 1992.

[11] G. C. Temes, "Exact computation of group delay and its sensitivities using adjoint network concept," *Electron. Lett.*, vol. 6, pp. 483–485, 1970.

[12] J. W. Bandler, M. R. M. Rizk, and H. Tromp, "Efficient calculation of group delay sensitivities," *IEEE Trans. Microwave Theory Tech.*, vol. MTT-24, pp. 188–194, 1976.

[13] C. M. Kudsia and V. O'Donovan, *Microwave Filters for Communications Systems*. Boston, MA: Artech House, 1974.

[14] J. Vlach, J. A. Barby, A. Vannelli, T. Talkhan, and C. J. Shi, "Group delay as an estimate of delay in logic," *IEEE Trans. Computer-Aided Design*, vol. 10, pp. 949–953, 1991.

[15] C. W. Ho, A. E. Ruehli, and P. A. Brennan, "The modified nodal approach to network analysis," *IEEE Trans. Circuits Systems*, vol. CAS-22, pp. 504–509, 1975.

[16] A. E. Ruehli, "Inductance calculations in a complex integrated circuit environment," *IBM J. Research and Development*, vol. 16, pp. 470–481, 1972.

[17] A. R. Djordjevic, R. F. Harrington, and T. K. Sarkar, *Matrix Parameters of Multiconductor Transmission Lines*. Boston, MA: Artech House, 1989.

[18] C. S. Walker, *Capacitance, Inductance and Crosstalk Analysis*. Boston: Artech House, 1990.

[19] J. W. Bandler, W. Kellermann and K. Madsen, "A superlinearly convergent minimax algorithm for microwave circuit design," *IEEE Trans. Microwave Theory Tech.*, vol. 33, pp. 1519–1530, 1985.

[20] J. W. Bandler and Q. J. Zhang, "Optimization techniques for modelling, diagnosis and tuning," *Analog Methods for Computer-Aided Circuit Analysis and Diagnosis*, T. Ozawa, Ed. New York, NY: Marcel Dekker, 1988, ch. 14.

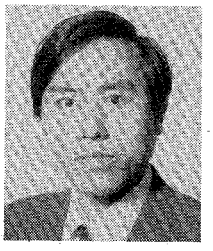

Ruolong Liu received the B.Eng. degree from the South Institute of Metallurgy, Jiangxi, China in 1982, the M.Eng. degree from Wuhan Iron and Steel University, Hubei, China, in 1988, both in electrical engineering.

He is currently working towards the Master degree at Carleton University, Ottawa, ON, Canada. His research interest is in the large scale simulation and optimization of electrical circuits.

Qi-jun Zhang (S'84–M'87) was born in Xianyan, Shanxi, China on October 8, 1959. He received the B.Eng. degree from the East China Engineering Institute, Nanjing, China in 1982, and the Ph.D. degree from McMaster University, Hamilton, Canada, in 1987, both in electrical engineering.

He was with the Institute of Systems Engineering, Tianjin University, Tianjin, China, from 1982 to 1983. He was a postdoctorate fellow in the Department of Electrical and Computer Engineering, McMaster University, in 1987 and 1988. He was a research engineer with Optimization Systems Associates Inc., Dundas, Ontario, Canada from 1988 to 1990. During 1989 and 1990 he was also an Assistant Professor (part-time) of Electrical and Computer Engineering in McMaster University. He joined the Department of Electronics, Carleton University, Ottawa, Canada in 1990 where he is presently an Assistant Professor. His professional interests include all aspects of circuit CAD with emphasis on large scale simulation and optimization, statistical design and modelling, parameter extraction, sensitivity analysis, and optimization of microwave circuits and high-speed VLSI interconnections.

Dr. Zhang is a contributor to *Analog Methods for Computer-Aided Analysis and Diagnosis*, (Marcel Dekker, 1988). Currently he is the holder of the Junior Industrial Chair in CAE established at Carleton University by Bell-Northern Research and the Natural Sciences and Engineering Research Council of Canada.

Michel S. Nakhla (S'73–M'76–SM'88) received the B.Sc. degree in electronics and communications from Cairo University, Egypt in 1967 and the M.A.Sc. and Ph.D. degrees in electrical engineering from Waterloo University, ON, Canada in 1973 and 1975, respectively.

During 1975, he was a Postdoctoral Fellow at University of Toronto, Ontario, Canada. In 1976 he joined Bell-Northern Research, Ottawa, Canada, as a member of the Scientific Staff where he became manager of the simulation group in 1980 and manager of the computer-aided engineering group in 1983. In 1988, he joined Carleton University, Ottawa, Canada, where he is currently a Professor in the Department of Electronics. His research interests include computer-aided design of VLSI and communication systems, high-frequency interconnects and synthesis of analog circuits. Currently he is the holder of the Computer-Aided Engineering Industrial Chair established at Carleton University by Bell Northern Research and the Natural Sciences and Engineering Research Council of Canada.